

Laser-phase-noise-induced stochastic-resonance fluorescence

A. A. Rangwala,* K. Wódkiewicz,[†] and C. Su

Center for Advanced Studies and Department of Physics and Astronomy, University of New Mexico, Albuquerque, New Mexico 87131

(Received 18 June 1990; revised manuscript received 30 July 1990)

Stochastic fluctuations of coherent and incoherent components of the resonance fluorescence intensity induced by Wiener-Levy laser phase noise are investigated. Statistical properties of the atomic dipole moment for different values of the laser linewidth and different strength of the driving field are calculated. The stochastic Mollow spectra of atomic dipole fluctuations are derived. It is shown that these spectra exhibit a triplet structure which is purely classical and entirely laser-noise dependent.

I. INTRODUCTION

In the presence of coherent radiation, resonant effects of a two-level atom can be described by the optical Bloch equations with two phenomenological lifetimes T_1 and T_2 .¹ If the environment of the radiating atom is a source of statistical perturbations described by a random noise with a finite coherent time, the optical Bloch equations have to be replaced by optical resonance equations with effective lifetimes dependent on the power of the driving radiation.² Power-dependent relaxations have been investigated both experimentally and theoretically in optical coherent transients.³

If the external fluctuations have a coherence time much shorter than any characteristic time scale of the resonant radiating atom it is possible to treat the external source of noise as a stochastic Gaussian white noise $x(t)$ with zero mean and the following autocorrelation:

$$\langle x(t)x(t') \rangle = 2\Gamma\delta(t-t'). \quad (1.1)$$

Laser-amplitude fluctuations, atomic dipole fluctuations, and atomic resonant-frequency fluctuations can all be incorporated in the stochastic Bloch equations with a multiplicative random noise. The stochastic Bloch equations can be written in all these cases in the form of the following matrix stochastic differential equation:⁴

$$\frac{dV}{dt} = [M_0 + ix(t)M]V, \quad (1.2)$$

where M_0 is the deterministic coherent part of the Bloch evolution and the matrix M describes the coupling of the Bloch variables with the external source of noise.

The stochastic differential Eq. (1.2) driven by the noise (1.1) can be averaged exactly and as a result the stochastic expectation value of $V(t)$ denoted here by $\langle V(t) \rangle$ satisfies the following differential equation:⁵

$$\frac{d\langle V(t) \rangle}{dt} = (M_0 - \Gamma M^2)\langle V(t) \rangle. \quad (1.3)$$

From this equation we see that the influence of the noise changes the coherent evolution by a simple additive damping term ΓM^2 . The solution of this equation can be written in the Laplace-transform form:

$$\langle V(t) \rangle = \oint dz \frac{1}{2\pi i} e^{zt} \langle \tilde{V}(z) \rangle,$$

where

$$\langle \tilde{V}(z) \rangle = (z - M_0 + \Gamma M^2)^{-1} \langle V(0) \rangle. \quad (1.4)$$

The time dependence of $\langle V(t) \rangle$ is determined by roots of the secular equation derived from (1.4). This secular equation gives the stochastic generalization of the well-known Torrey equation.¹ In all of the physical examples that we have mentioned above it is possible to show that the additional damping leads to so-called "substitution rules." In such cases we can derive certain exact rules explaining how to add the nonradiative (noise-induced) lifetimes to T_1 and T_2 . For example, if atomic dipole frequency fluctuations are investigated, the substitution rules lead to a broadening of the transverse rate, leaving an unchanged longitudinal rate:

$$\frac{1}{T_2} = \frac{A}{2} + \Gamma, \quad \frac{1}{T_1} = A. \quad (1.5)$$

There is, however, a very important case of white-noise fluctuations that escapes this general scheme. This is the Wiener-Levy diffusion of laser phase $\phi(t)$ leading to white-noise fluctuations of the instantaneous laser frequency $\mu(t) = \dot{\phi}(t)$:

$$\langle \mu(t)\mu(t') \rangle = 2\Gamma\delta(t-t'). \quad (1.6)$$

At a first glance it may seem strange to have difficulties with laser-frequency fluctuations when atomic frequency fluctuations lead to an almost trivial result (1.4). After all, both the laser frequency ω_L and the atomic frequency ω_0 enter the Bloch equations via the detuning $\Delta = \omega_0 - \omega_L$ in a completely symmetric way. The fundamental differences between frequency fluctuations of the atomic dipole or of the laser electric field can be traced back to the interaction Hamiltonian. From the structure of this Hamiltonian it is clear that fluctuations of ω_0 influence diagonal atomic transitions, while fluctuations in ω_L involve all the off-diagonal atomic transitions. The symmetry of these fluctuations at the level of the atomic detuning has been obtained with the help of a rotating frame, rotating with a random frequency $\mu(t)$. In fact, from some very early investigations it follows that it is impossi-

ble to find one universal rotating frame in which both atomic populations and atomic coherence can be driven by laser fluctuations in the form described by the canonical stochastic equation (1.2).^{5,6} This relatively simple fact has important physical consequences. With laser-frequency fluctuations we have, in fact, two different and distinct rotating frames leading to the stochastic equation (1.2). The first frame is used to describe the atomic populations and the resulting incoherent component of the resonance fluorescence. The second frame is used to describe the atomic dipole moments and the resulting coherent (Rayleigh) component of the strong-field resonance fluorescence.

Even though most of the theoretical tools and results relevant for this problem had been developed several years ago, it is only just recently that the first experiment has been reported in which the noise-induced mean and variance of the total fluorescence intensity have been measured.⁷

In view of these very important experiments it is the purpose of this paper to examine the problem of laser-frequency noise-induced fluctuations of the coherent $I_{\text{coh}}(t)$ and incoherent $I_{\text{inc}}(t)$ fluctuations in resonance fluorescence. Possible future measurements of the fluctuations of the coherent intensity could exhibit the striking property of the failure of the substitution "rules" in the laser-frequency noise described just by a simple white noise (no cutoff effects due to a possible finite coherence of the frequency noise).

As we have said before, the relevant steps of the statistical average have been published in several papers in the past. This allows us to keep all the technical arguments at a minimum level throughout this paper.

This paper is organized as follows. In Sec. II we introduce the stochastic Bloch equations with Wiener-Levy laser-frequency fluctuations and define the coherent and the incoherent components of the resonance-fluorescence intensity. In Sec. III we discuss the physical properties of statistically averaged coherent and incoherent resonance-fluorescence intensity components. In Sec. IV we derive the power spectrum of laser-noise-induced atomic dipole fluctuations. This purely classical spectrum exhibits ac Stark splitting for strong laser excitations. In Sec. V we present the optical resonance equations for the mean atomic population and the mean atomic dipole moment in the presence of laser noise. Effective power and laser-noise-dependent transverse and longitudinal lifetimes are derived and discussed. Finally, some concluding remarks are given in Sec. VI.

II. STOCHASTIC BLOCH EQUATIONS

The stochastic Bloch equations (with quantum averages already performed) have the following form:¹

$$\dot{d} = \left[-i\Delta - \frac{A}{2} \right] d - i\frac{\Omega}{2} e^{-i\phi(t)} w, \quad (2.1a)$$

$$\dot{d}^* = \left[i\Delta - \frac{A}{2} \right] d^* + i\frac{\Omega}{2} e^{i\phi(t)} w, \quad (2.1b)$$

$$\dot{w} = -A(1+w) + i\Omega(d^* e^{-i\phi(t)} - d e^{i\phi(t)}), \quad (2.1c)$$

where $u = d + d^*$, $v = i(d - d^*)$, and w are three components of the Bloch vector driven by a stochastic field with constant Rabi frequency Ω and fluctuating phase $\phi(t)$. The radiative damping and detuning are denoted by the Einstein A coefficient and Δ , respectively. Phase fluctuations of the laser light are assumed to be described by a Wiener-Levy stochastic process leading to frequency fluctuations characterized by the autocorrelation function (1.6).

It is well known that the total resonance-fluorescence intensity I consists of two contributions:⁸

$$I = I_{\text{coh}} + I_{\text{inc}}. \quad (2.2)$$

The first one, originating from the motion of the dipole $d(t)$, driven by the laser field, is sometimes called the coherent or the Rayleigh scattered intensity:

$$I_{\text{coh}}(t) = d^*(t)d(t). \quad (2.3)$$

The second one, called the incoherent intensity, is due to the quantum fluctuations of the dipole moment produced by the vacuum field.

The total resonance-fluorescence intensity is determined by the atomic population $p(t) = w(t) + 1/2$ of the radiating two-level atom as a result we obtain that

$$I = p(t) \quad (2.4)$$

and

$$I_{\text{inc}} = p(t) - d^*(t)d(t). \quad (2.5)$$

If the external stochastic fluctuations of the field, for example laser-frequency noise, are included, the resonance-fluorescence intensities I , I_{inc} , and I_{coh} become random statistical variables for which means, variances, and noise power spectra can be calculated and measured. In recent experiments the statistical properties of the atomic population fluctuations have been measured.⁷

In this paper we shall be concerned mainly with the statistical properties of resonance fluorescence generated by the atomic dipole fluctuations:

$$\langle I_{\text{coh}} \rangle = \langle d^*(t)d(t) \rangle, \quad (2.6a)$$

$$\langle I_{\text{inc}} \rangle = \langle p(t) \rangle - \langle d^*(t)d(t) \rangle. \quad (2.6b)$$

The statistical properties of the total fluorescence I are fully described by the atomic population fluctuations, while the coherent and incoherent part of the fluorescence involves the dipole-moment fluctuations.

Whenever fluctuations of a randomly distributed function [$p(t)$ or $d(t)$] are detected and observed it is interesting to calculate and to measure the power spectrum of the noise.

For steady-state autocorrelations of population and dipole we define the following quantities:

$$S_p(\omega) = \lim_{t \rightarrow \infty} 2 \operatorname{Re} \int_0^\infty e^{-i\omega\tau} \langle p(t+\tau)p(t) \rangle d\tau, \quad (2.7)$$

$$S_d(\omega) = \lim_{t \rightarrow \infty} 2 \operatorname{Re} \int_0^\infty e^{-i(\omega-\omega_0)\tau} \langle d^*(t+\tau)d(t) \rangle d\tau. \quad (2.8)$$

The quantity $S_p(\omega)$ represents a stationary spectrum of

population fluctuations, while $S_d(\omega)$ represents the stationary spectrum of dipole fluctuations.

III. RESONANCE FLUORESCENCE INTENSITY

The transformation of the stochastic Bloch equations (2.1) into the canonical form (1.2) is well known and has

$$V^T(t) = (I_{\text{coh}}(t), d(t)w(t)e^{i\phi(t)}, d^*(t)w(t)e^{-i\phi(t)}, d^2(t)e^{2i\phi(t)}, d^{*2}(t)e^{-2i\phi(t)}, w^2(t), d(t)e^{i\phi(t)}, d^*(t)e^{-i\phi(t)}, I(t), A). \quad (3.1)$$

By a repeated application of the stochastic Bloch equations (2.1) it is easy to check that this ten-component vector satisfies a stochastic differential equation in a form given by (1.2) with proper time-independent 10×10 matrices M_0 and M . As a result we obtain that the stochastic expectation value of $V(t)$ has to satisfy Eq. (1.3) which has the explicit Laplace-transform form solution given by Eq. (1.4). In the following we shall only be interested in steady-state values of averaged fluorescence intensities. Isolating the pole at $z=0$ and evaluating the corresponding residue, we obtain after a simple but lengthy algebra the following expressions:

$$\langle I_{\text{coh}}(\infty) \rangle = \frac{A\Omega^2}{2} \frac{\text{Re}\{[(\mathcal{L}_1^{-1}\mathcal{L}_2\mathcal{L}_3)^*]^{-1}[(\mathcal{L}_2\mathcal{L}_3)^{-1} + \frac{1}{2}\Omega^2]\}}{[\Omega^2\text{Re}(\mathcal{L}_1) - A]\{A|(\mathcal{L}_2\mathcal{L}_3)^{-1} + \frac{1}{2}\Omega^2|^2 - 2\Omega^2\text{Re}[\mathcal{L}_3^*]^{-1}[(\mathcal{L}_2\mathcal{L}_3)^{-1} + \frac{1}{2}\Omega^2]\}} \quad (3.2a)$$

and

$$\langle I \rangle = \frac{1}{2} \frac{\Omega^2\text{Re}(\mathcal{L}_1)}{\Omega^2(\text{Re}\mathcal{L}_1) - A}, \quad (3.2b)$$

where the complex Lorentzian functions $\mathcal{L}_1(\Delta)$, $\mathcal{L}_2(\Delta)$, and $\mathcal{L}_3(\Delta)$ are defined by the following expressions: $\mathcal{L}_1 = (i\Delta - \frac{1}{2}A - \Gamma)^{-1}$, $\mathcal{L}_2 = (i\Delta - \frac{1}{2}3A - \Gamma)^{-1}$, $\mathcal{L}_3 = (i\Delta - \frac{1}{2}A - 2\Gamma)^{-1}$. For later reference we also note that

$$\langle wde^{i\phi}(\infty) \rangle = -\frac{2i\mathcal{L}_3^*{}^{-1}}{\Omega} \langle d^2e^{2i\phi}(\infty) \rangle, \quad (3.2c)$$

$$\langle d^2e^{2i\phi}(\infty) \rangle = \frac{A^2\Omega^2}{2} \frac{\{(1 - A\mathcal{L}_1^*)[(\mathcal{L}_2\mathcal{L}_3)^{-1} + \frac{1}{2}\Omega^2] - 2i\Omega^2\mathcal{L}_3^{-1}\text{Im}\mathcal{L}_1\}}{[\Omega^2\text{Re}\mathcal{L}_1 - A]\{A|(\mathcal{L}_2\mathcal{L}_3)^{-1} + \frac{1}{2}\Omega^2|^2 - 2\Omega^2\text{Re}\{\mathcal{L}_3^*]^{-1}[(\mathcal{L}_2\mathcal{L}_3)^{-1} + \frac{1}{2}\Omega^2]\}}, \quad (3.2d)$$

$$\langle de^{i\phi}(\infty) \rangle = \frac{iA\Omega}{2} \frac{\mathcal{L}_1^*}{\Omega^2\text{Re}\mathcal{L}_1 - A}. \quad (3.2e)$$

It is easy to check that in the limit of weak field, i.e., when $\Omega \ll A, \Gamma$ we obtain that the total fluorescence is equal to the coherent contribution and the incoherent part vanishes:

$$\langle I \rangle \cong \langle I_{\text{coh}} \rangle = \frac{\Omega^2}{2A} \frac{\frac{1}{2}A + \Gamma}{(\frac{1}{2}A + \Gamma)^2 + \Delta^2}. \quad (3.3)$$

In this limit it is justified to speak about substitution rules which are described by the Lorentzian function $\mathcal{L}_1(\Delta)$ which leads to Eq. (1.5), and as a consequence are equivalent to the substitution rules obtained for atomic-frequency fluctuations. In the limit of weak field, laser-frequency fluctuations and atomic dipole fluctuations are indistinguishable. The situation is completely different if the field is strong. In this case the rotating frame leading to the ten-component vector (3.1) involves three Lorentzian functions forming the expression (3.2a). Because of this the substitution rules (1.5) are not even valid approximately, and the fluorescence intensities $\langle I_{\text{coh}} \rangle$ and $\langle I \rangle$ have to be described by the full expressions given by Eqs. (3.2) with three distinct functions \mathcal{L}_1 , \mathcal{L}_2 , and \mathcal{L}_3 .

In Fig. 1 we have plotted the total and the coherent in-

been described in great detail elsewhere.^{6,5,9}

In this paper we shall just quote the main result of this transformation when applied to the problem of coherent and incoherent intensity fluctuations induced by white-noise laser-frequency noise.

We introduce the following ten-component stochastic vector [transposed of $V(t)$]:

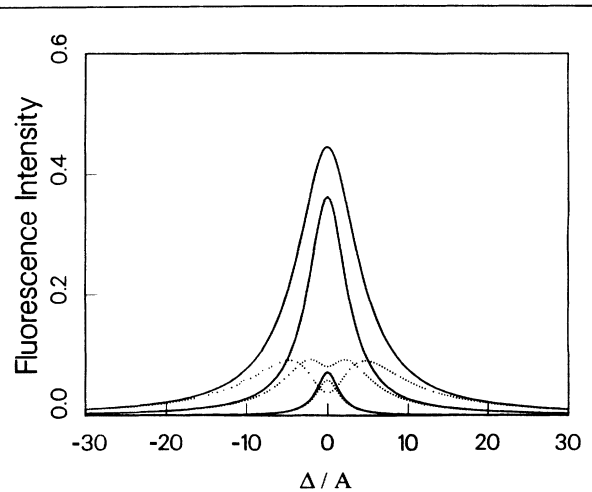


FIG. 1. Total fluorescence $\langle I \rangle$ and coherent fluorescence $\langle I_{\text{coh}} \rangle$ as a function of laser detuning Δ with $\Gamma = 1A$. The different solid lines from the bottom to the top correspond to the total fluorescence with $\Omega = 0.5, 2.0,$ and $3.5A$. The different dotted lines correspond to the coherent fluorescence. The smallest Lorentzian curve corresponds to $\Omega = 0.5A$. The curve with a shallow dip corresponds to $\Omega = 2.0A$. The curve with the most pronounced dip corresponds to $\Omega = 3.5A$.

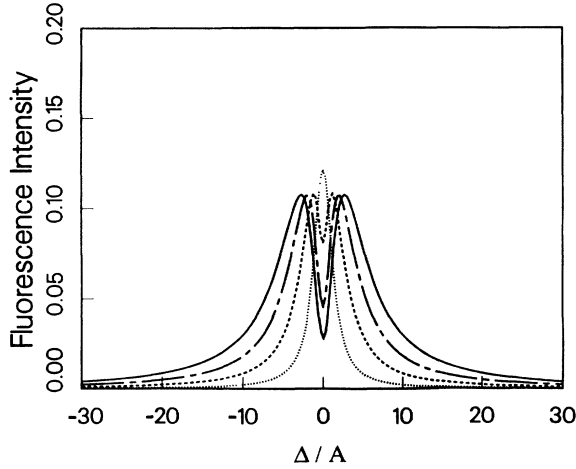


FIG. 2. Coherent fluorescence $\langle I_{\text{coh}} \rangle$ as a function of laser detuning Δ with $\Gamma=0.2A$. The dotted line corresponds to $\Omega=0.8A$. The dashed line corresponds to $\Omega=1.6A$. The dash-dotted line corresponds to $\Omega=2.4A$. The solid line corresponds to $\Omega=3.2A$.

tensity fluorescence as a function of the detuning for different values of Γ and Ω . In all the plots in this paper, Δ , Γ , ω , and Ω are expressed in units of the natural lifetime A . We see that for $\Omega=0.5A$ and $\Gamma=1A$, the coherent fluorescence is practically identical to the total fluorescence. For higher values of the Rabi frequency, i.e., for $\Omega=2$ and $3.5A$ the differences between these two fluorescence components are more pronounced. Note that for $\Omega=2A$ the curves for both $\langle I \rangle$ and $\langle I_{\text{coh}} \rangle$ have a dip at the exact resonance $\Delta=0$.

In Fig. 2 we have plotted the coherent fluorescence intensity for different Rabi frequencies ($\Omega=0.8, 1.6, 2.4$, and $3.2A$) and for a small laser linewidth $\Gamma=0.2A$. We note that for $\Omega > 1$ the intensity has a well-pronounced

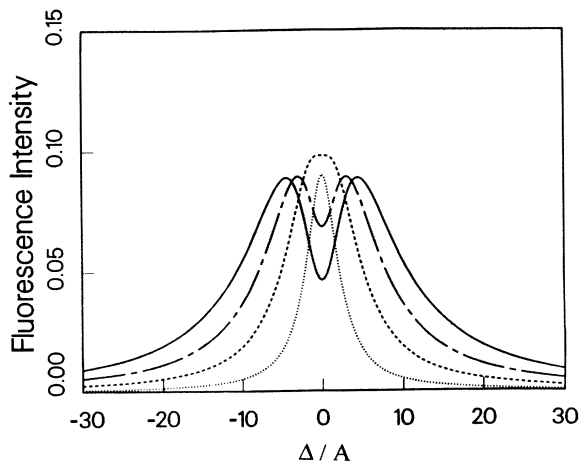


FIG. 3. Coherent fluorescence $\langle I_{\text{coh}} \rangle$ as a function of laser detuning Δ with $\Gamma=1.2A$. The dotted line corresponds to $\Omega=0.8A$. The dashed line corresponds to $\Omega=2.4A$. The dash-dotted line corresponds to $\Omega=3.2A$. The solid line corresponds to $\Omega=1.6A$.

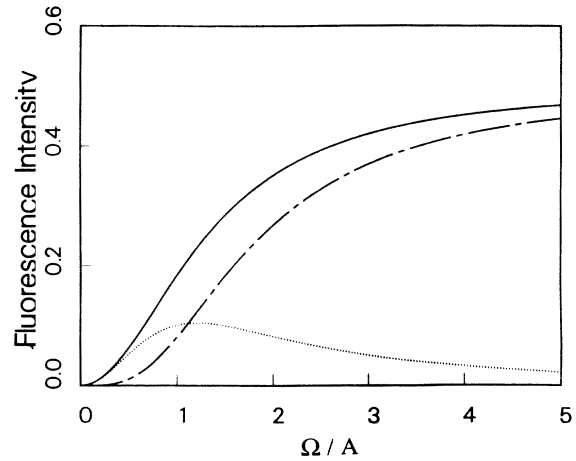


FIG. 4. Intensity fluorescence as a function of Rabi frequency at exact resonance $\Delta=0$ and $\Gamma=1.2A$: total intensity $\langle I \rangle$ (solid line), coherent intensity $\langle I_{\text{coh}} \rangle$ (dotted line), incoherent intensity $\langle I_{\text{inc}} \rangle$ (dash-dotted line).

Lorentzian dip at exact resonance. In Fig. 3 we have plotted the corresponding curves from Fig. 2 but with a larger laser linewidth $\Gamma=1.2A$. The dips are still there except that they have been much broadened by the laser linewidth.

In Fig. 4 we have plotted the total, coherent, and incoherent fluorescence intensities as functions of Rabi frequency Ω for $\Delta=0$ and $\Gamma=1.2$. We note in this figure the well-known fact that the coherent (Rayleigh) component of the fluorescence intensity peaks and then falls off with increasing power of the laser light.⁸

IV. POWER SPECTRA OF DIPOLE FLUCTUATIONS

As we pointed out before, phase-noise-induced fluctuations of the population $p(t)$ lead to the total resonance-fluorescence intensity $\langle I \rangle$. Correlations of population fluctuations [see Eq. (2.7)] have been investigated for low-intensity fields several years ago.¹⁰ Recently calculations of these fluctuations and their power spectra for large values of Ω have been published.¹¹

It is the purpose of this section to study the power spectra of dipole-moment fluctuations responsible for the coherent fluorescence intensity. The quantum correlations of atomic dipole moments lead to the well-known Mollow spectrum.⁸ Because we are dealing in this paper with purely classical fluctuations of the Bloch variables, the power spectra of dipole correlations describe the power spectrum of a radiating classical dipole moment. Because in this case correlations of the classical dipole are induced by stochastic fluctuations of the driving field, we shall call the resulting power spectrum a stochastic Mollow spectrum (SMS).

In order to calculate the dipole-dipole correlations required in the definition (2.8) of the dipole power spectrum, we introduce the following four-component transposed vector:

$$V^T(t, \tau) = (d^*(t + \tau)d(t), w(t + \tau)d(t)e^{i\phi(t + \tau)}, d(t + \tau)d(t)e^{2i\phi(t + \tau)}, d(t)e^{i\phi(t)}) . \quad (4.1)$$

By a repeated application of the stochastic Bloch equations (2.1) it is easy to check that this four-component vector satisfies a stochastic differential equation in a form given by (1.2) with proper time-independent 4×4 matrices M_0 and M , and the following initial condition for $\tau=0$:

$$V^T(t, \tau=0) = (I_{\text{coh}}(t), w(t)d(t)e^{i\phi(t)}, d^2(t)e^{2i\phi(t)}, d(t)e^{i\phi(t)}) . \quad (4.2)$$

In the steady-state limit, the dipole-moment autocorrelation can be calculated using the procedure described in the previous sections and noting that the steady-state values of (4.2) are given by the first, second, fourth, and seventh components of the vector (3.1). Combining these results, we obtain the following exact expression for the SMS in the presence of laser-phase fluctuation:¹²

$$S_d(\omega) = 2 \operatorname{Re} \left[\frac{N_1(\omega - \omega_0)\psi_1 + N_2(\omega - \omega_0)\psi_2 + N_3(\omega - \omega_0)\psi_3 + N_4(\omega - \omega_0)\psi_4}{N(\omega - \omega_0)} \right] , \quad (4.3)$$

where the four functions N_i in the numerator are defined by the following relations:

$$N_1(\omega) = (i\omega + \Gamma) \left[(i\omega + A + \Gamma) \left[i\omega + i\Delta + \frac{A}{2} + 4\Gamma \right] + \frac{\Omega^2}{2} \right] , \quad (4.4a)$$

$$N_2(\omega) = \frac{i\Omega}{2} \left[\left[i\omega + i\Delta + \frac{A}{2} + 4\Gamma \right] (i\omega + \Gamma) \right] , \quad (4.4b)$$

$$N_3(\omega) = \frac{\Omega^2}{2} (i\omega + \Gamma) , \quad (4.4c)$$

$$N_4(\omega) = -i \frac{A\Omega}{2} \left[i\omega + i\Delta + \frac{A}{2} + 4\Gamma \right] , \quad (4.4d)$$

and where the denominator function is

$$N(\omega) = (i\omega + \Gamma) \left[\left[i\omega - i\Delta + \frac{A}{2} \right] (i\omega + A + \Gamma) \left[i\omega + i\Delta + \frac{A}{2} + 4\Gamma \right] + \Omega^2 \left[i\omega + \frac{A}{2} + 2\Gamma \right] \right] . \quad (4.4e)$$

In the formula (4.3) the four functions $\psi_i = \lim_{t \rightarrow \infty} \langle V_i(t, \tau=0) \rangle$ are the steady-state expectation values of the four components ($i=1, \dots, 4$) of the vector (4.2) and are explicitly given by Eqs. (3.2a) and (3.2c)–(3.2e). Note that the expression for the SMS involves, in addition to the two complex Lorentzian functions \mathcal{L}_1 and \mathcal{L}_3 , an additional Lorentzian $\mathcal{L}_4 = (i\Delta + \frac{1}{2}A + 4\Gamma)^{-1}$.

In the limit of weak field the SMS becomes identical with the quantum Weisskopf-Heitler spectrum of resonance fluorescence with the laser linewidth contribution.¹³ In the limit of weak field, the two-level atom becomes a classical harmonic oscillator, and statistical correlations of the atomic dipole moment are linearly dependent on the electric-field autocorrelation function. If the field is purely monochromatic, the Weisskopf-Heitler resonance fluorescence consists of a sharp peak centered at the driving field.⁸ If the external field fluctuates and has finite linewidth Γ , the standard Weisskopf-Heitler spectrum is modified. At exact resonance, the Rayleigh peak has a bandwidth equal to Γ . Off resonance, the spectrum has an additional component centered around the atomic frequency ω_0 , with a bandwidth equal to the natural linewidth of the excited state. The height of this peak is proportional to the laser linewidth Γ . The fact that incoherent effects introduce an additional nonelastic component in the fluorescence spectrum has

been predicted¹⁴ and observed experimentally¹⁵ for a completely different physical situation involving atomic collisions.

In Fig. 5 we have plotted the SMS for weak-field excitation $\Omega=0.2A$, detuned by $\Delta=10A$ and with a laser

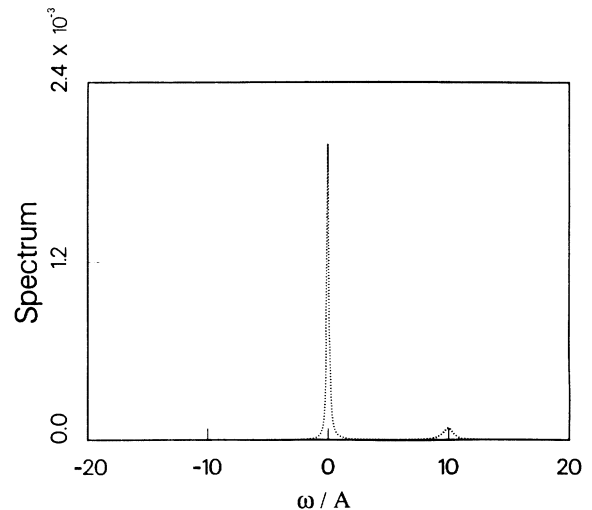


FIG. 5. The SMS for weak field $\Omega=0.2A$, $\Delta=10A$, and $\Gamma=0.1A$.

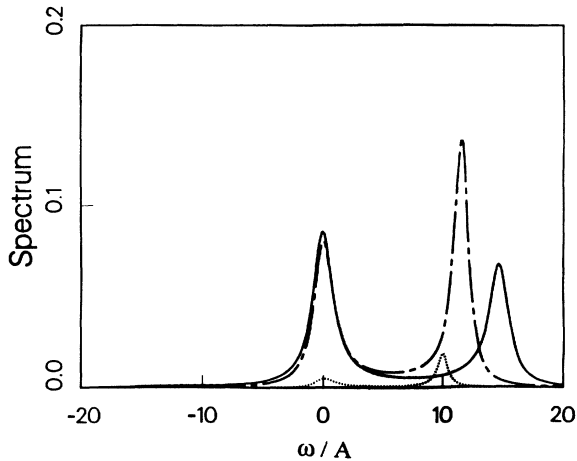


FIG. 6. The SMS for $\Gamma=1.0A$ and $\Delta=10A$. The dotted line corresponds to the spectrum with $\Omega=1A$. The dash-dotted line corresponds to the spectrum with $\Omega=6A$. The solid line corresponds to the spectrum with $\Omega=11A$.

linewidth $\Gamma=0.1A$. We see that in addition to the Rayleigh component centered around $\omega=\omega_L$ we have a purely inelastic component centered around $\omega=\omega_0$. In Fig. 6 we have plotted the same spectrum for a driving field detuned by $\Delta=10A$ with a laser linewidth $\Gamma=1A$ and three different values of the Rabi frequency $\Omega=1, 6$, and $11A$. We see that with increased laser linewidth and increased Rabi oscillation the inelastic peak can be higher compared to Fig. 5 and even shifted from its atomic frequency ω_0 .

In Fig. 7 we have compared the power spectrum of population fluctuations¹¹ with the SMS for weak field $\Omega=0.15A$, detuned by $\Delta=3A$ and a small laser

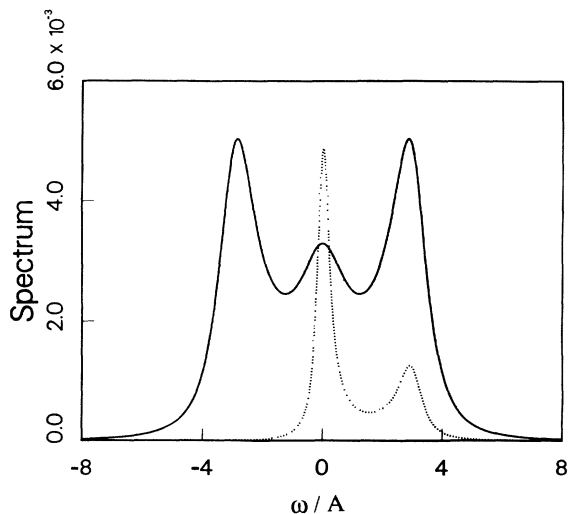


FIG. 7. Comparison of the coherent part of the fluorescence spectrum (dotted line) with the total spectrum (solid line) for $\Gamma=0.25A$, $\Delta=3A$, and $\Omega=0.15A$. In order to normalize the coherent and the total spectrum to the same height, the population spectrum has been magnified by a factor 2×10^4 .

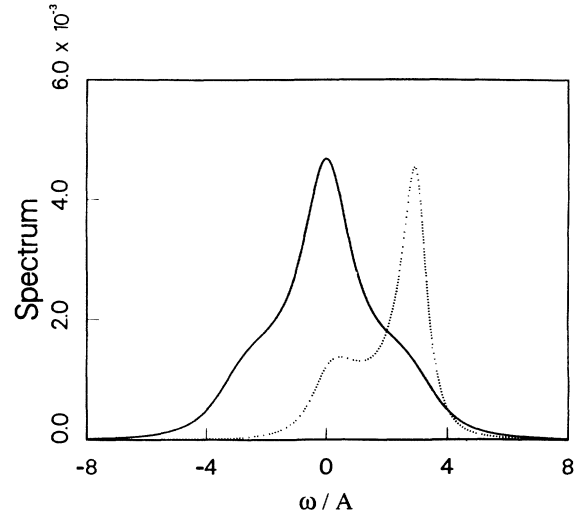


FIG. 8. The same as Fig. 7 but with $\Gamma=1A$. The population spectrum has been magnified by a factor 2.8×10^3 .

linewidth $\Gamma=0.25A$. It should be noted that in the weak limit, the population power spectrum is of the order Ω^4 , while the dipole-moment power spectrum is of the order Ω^2 . Because of this we have normalized the spectra to the same height. This normalization leads to a magnification of the population spectrum. The magnification factor is given in the figure captions. In Fig. 8 we have the same comparison, except that the laser linewidth is now $\Gamma=1A$.

A remarkable feature of the SMS emerges when the Rabi oscillation is considerably increased. In Fig. 9 we

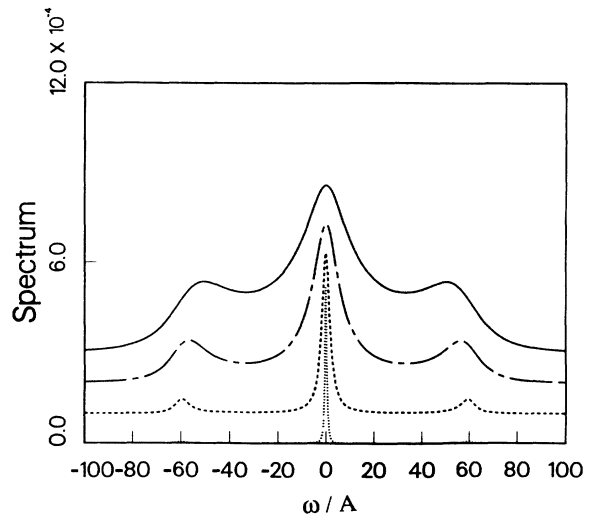


FIG. 9. The SMS for $\Omega=60A$, $\Delta=0$ and different values of laser linewidth. The dotted line corresponds to $\Gamma=0.5A$. The dashed line corresponds to $\Gamma=2.0A$ (the figure has been shifted by 0.0001 and magnified by 3.0). The dash-dotted line corresponds to $\Gamma=6.0A$ (the figure has been shifted by 0.0002 and magnified by 6.0). The solid line corresponds to $\Gamma=10A$ (the figure has been shifted by 0.0003 and magnified by 7.5).

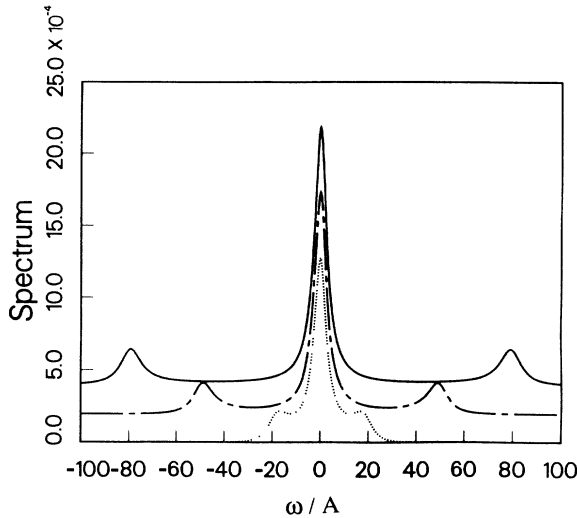


FIG. 10. The SMS for $\Delta=0$ and $\Gamma=3A$. The dotted line corresponds to $\Omega=20A$. The dash-dotted line corresponds to $\Omega=50A$ (the figure has been shifted by 0.0002 and magnified by 8.0). The solid line corresponds to $\Omega=80A$ (the figure has been shifted by 0.004 and magnified by 24.0).

have plotted the dipole-moment spectrum for $\Omega=60A$, at exact resonance and for different four values of the laser linewidth: $\Gamma=0.5, 2.0, 6.0,$ and $10A$. In order to exhibit more clearly the structure of the SMS we have shifted and magnified the curves by factors explained in the figure caption. The remarkable feature of these curves is the presence of a triplet. Note that the appearance of these three peaks is similar to the structure of the famous

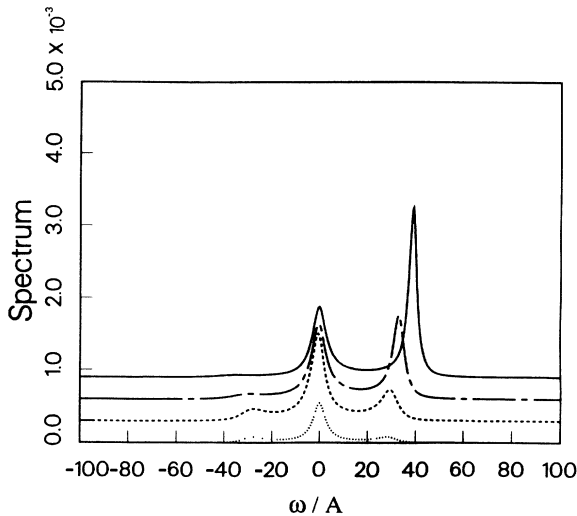


FIG. 11. The SMS for $\Gamma=3A$, $\Omega=30A$ for different values of detuning. The dotted line corresponds to $\Delta=0$. The dashed line corresponds to $\Delta=5A$ (the figure has been shifted by 0.0003). The dash-dotted line corresponds to $\Delta=15A$ (the figure has been shifted by 0.0006 and reduced by 5.0). The solid line corresponds to $\Delta=25A$ (the figure has been shifted by 0.0009 and reduced by 10.0).

Mollow spectrum. The fundamental difference between the stochastic spectrum and the quantum spectrum is in the source of fluctuations. The Mollow spectrum results from vacuum fluctuations, while the SMS results from phase-laser fluctuations. We see that when Γ is small, there is basically one central Rayleigh peak, but when Γ increases, two sideband peaks appear and their heights grow with Γ . This indicates that the triplet structure is purely noise dependent. Correlations of the atomic dipole result in this case from purely classical fluctuations induced by the laser-phase noise. In Fig. 10 we have plotted the SMS for $\Delta=0$ and $\Gamma=3A$ but for different values of the Rabi frequency Ω in order to exhibit the stochastic ac Stark frequency splitting of the dipole-moment power spectrum. In Fig. 11 we have plotted the SMS for $\Gamma=3A$, $\Omega=30A$ but detuned by $\Delta=0, 5, 15,$ and $25A$. Comparing these curves with the triplet at exact resonance, we see that detuning introduces a strong asymmetry in the atomic dipole-moment noise power spectrum.

V. OPTICAL RESONANCE EQUATIONS WITH PHASE NOISE

The optical resonance equations (ORE) are a substitute for the optical Bloch equations in cases when the relaxation mechanism becomes power and detuning dependent. It has been shown several years ago that a large class of broadening mechanisms described by external fluctuations with a finite coherence time can be represented by the ORE with power- and detuning-dependent homogeneous lifetimes T_1 and T_2 .² We have already pointed out that the Weiner-Levy fluctuations of the laser lead to two distinct rotating frames for the Bloch vector. In these frames the stochastic Bloch equations have the canonical form given by Eq. (1.2).

In this section we shall apply the idea of the ORE in order to derive effective homogeneous lifetimes T_1 and T_2 for the stochastic expectation values of the atomic inversion $\langle w(t) \rangle$ and the atomic dipole moment $\langle d(t) \rangle$.

The different rotating frames for $w(t)$ and $d(t)$ are reflected in the existence of two distinct vectors $V(t)$ involving the inversion and the dipole that form Eq. (2.1) with different matrices M_0 and M .

The following four-component vector [transposed of $V(t)$] contains $w(t)$ and has no $d(t)$ in its definition:

$$V^T(t) = (w(t), d^*(t)e^{-i\phi(t)}, d(t)e^{i\phi(t)}, A). \quad (5.1)$$

The following four-component vector [transposed of $V(t)$] contains $d(t)$ and has no $w(t)$ in its definition:

$$V^T(t) = (d(t), e^{-i\phi(t)}w(t), d^*(t)e^{-2i\phi(t)}, e^{-i\phi(t)}). \quad (5.2)$$

The stochastic vector (5.1) defines population fluctuations, while the stochastic vector (5.2) defines atomic fluctuations. Note that the stochastic evolutions of (5.1) and (5.2) are completely independent, and as a result the stochastic averages in the form given by Eq. (1.3) are different because they involve different matrices M_0 and M .

The ORE are in general derived from such averaged

equations by an adiabatic elimination of the laser-damped components of the vector $\langle V(t) \rangle$. This procedure is justified for values of $\Gamma \geq A$ and for times when the early transients have died out. This procedure is exact at steady state. Performing the adiabatic elimination of the damped variables in the two vectors (5.1) and (5.2), we obtain the ORE for the average dipole transition and the average inversion in the following form:

$$\langle \dot{d} \rangle = \left[-i\Delta - \frac{A}{2} \right] \langle d \rangle + \frac{\Omega^2(i\Delta - \frac{1}{2}A - 4\Gamma)}{\Omega^2 - 2(A + \Gamma)(i\Delta - \frac{1}{2}A - 4\Gamma)} \langle d \rangle, \quad (5.3a)$$

$$\langle \dot{w} \rangle = - \left[A + \frac{\Omega^2}{2} \frac{(A + 2\Gamma)}{(\frac{1}{2}A + \Gamma)^2 + \Delta^2} \right] \langle w \rangle - A. \quad (5.3b)$$

These ORE are diagonal and decoupled from each other. From Eq. (5.3b) for the atomic inversion we can conclude that the decay of the mean population is governed by an effective longitudinal linewidth given by

$$\frac{1}{T_2^w} = A + \frac{\Omega^2}{2} \frac{(A + 2\Gamma)}{(\frac{1}{2}A + \Gamma)^2 + \Delta^2}. \quad (5.4)$$

This expression has a power-dependent and laser-dependent contribution which has a Lorentzian shape.

The dynamical equation for the atomic dipole moment contains the complex Lorentzian function \mathcal{L}_4 , typical in the expression for the SMS [see Eqs. (4.4)]. From Eq. (5.3a) we obtain that the dipole moment oscillates with an effective detuning:

$$\Delta_{\text{eff}} = \Delta - \text{Im}\{[\mathcal{L}_4(\Delta) - 2(A + \Gamma)/\Omega^2]^{-1}\}, \quad (5.5a)$$

and decays with an effective transverse lifetime given by

$$\frac{1}{T_2^d} = \frac{A}{2} + \text{Re}\{[\mathcal{L}_4(\Delta) - 2(A + \Gamma)/\Omega^2]^{-1}\}. \quad (5.5b)$$

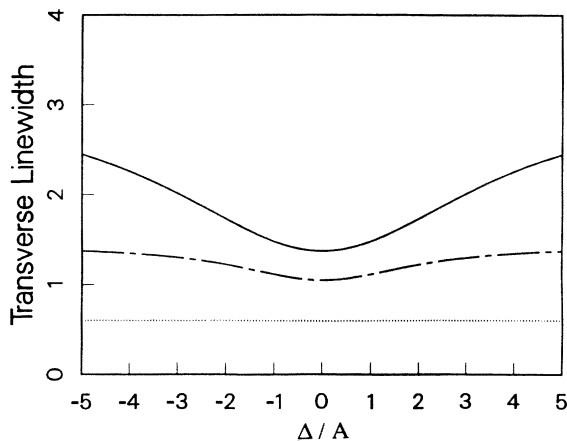


FIG. 12. Plots of the effective transverse lifetime as a function of the atomic detuning for $\Gamma=0.2A$ and different values of Rabi oscillation. The dotted line corresponds to $\Omega=0.5A$. The dash-dotted line corresponds to $\Omega=1.5A$. The solid line corresponds to $\Omega=2.5A$.

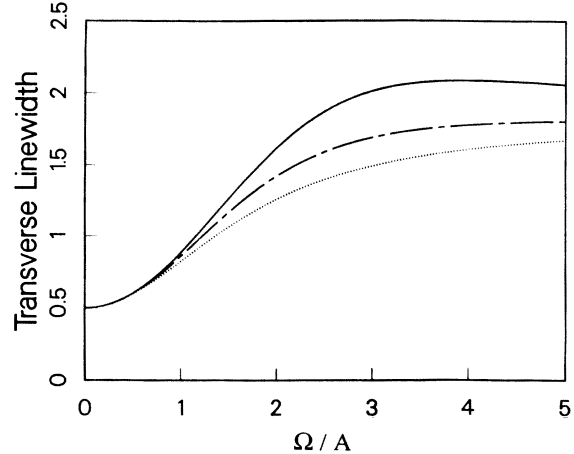


FIG. 13. Plots of the effective transverse lifetime as a function of the Rabi oscillation for $\Gamma=0.2A$ and different values of the atomic detuning. The dotted line corresponds to $\Delta=0.5A$. The dash-dotted line corresponds to $\Delta=1.5A$. The solid line corresponds to $\Delta=2.5A$.

In Fig. 12 we have plotted the dipole effective lifetime (5.5b) as a function of the detuning for $\Gamma=0.2A$ and three values of Rabi frequency: $\Omega=0.5, 1.5, \text{ and } 2.5A$. Note that this effective transverse linewidth has a power-dependent dip located at exact resonance. In Fig. 13 we have plotted the same transverse lifetime as a function of Rabi frequency with a laser bandwidth $\Gamma=0.2A$ and three different values of the detuning $\Delta=0.5, 1.5, \text{ and } 2.5A$. With increased laser noise the detuning dependence of the transverse lifetime becomes less pronounced.

VI. CONCLUSION

The theoretical investigations of this work have been stimulated by a recent experiment⁷ in which fluorescence from a large number of atoms (typically of the order of 10^5) has been observed by a detector with an area much larger than the coherence of the fluorescence light with fluctuating phase. The fluorescence detected in this experiment has been purely classical due to the large number of radiating atoms, and the measured fluctuations of light intensity have been induced by classical laser-phase fluctuations.

Our theoretical investigations of resonance fluorescence induced by Weiner-Levy laser-phase fluctuations have been extended to the forward or incoherent components of scattered light. In contrast to the total fluorescence, the incoherent part of the scattered light is mostly governed by the atomic dipole moment, which plays the dominant role in the forward light scattering.

We have investigated the coherent and the incoherent components of the fluorescence intensity, induced by laser-phase noise. We have compared the coherent and the incoherent fluorescence for different values of Rabi frequency and laser-phase bandwidth. We have calculated the power spectrum of laser-noise-induced dipole fluctuations. This purely classical spectrum exhibits several

interesting features not observed in atomic population fluctuations. We have calculated this spectrum for different values of atomic detuning, Rabi oscillation, and laser-phase bandwidth. We have shown that for weak-field excitations, this spectrum is identical with the well-known Weisskopf-Heitler spectrum. For strong laser excitations, we have shown that the SMS exhibits a purely noise-dependent triplet structure.

Finally, we have derived the optical resonance equations for the atomic population and the atomic dipole moment in the presence of laser-phase noise. We have shown that the ORE have effective transverse and longitudinal lifetimes which are detuning and power dependent.

In view of recent experiments, we believe that the laser-phase noise-induced stochastic properties of reso-

nance fluorescence involving forward light scattering and the SMS could be investigated for different values of the laser bandwidth and laser intensity.

ACKNOWLEDGMENTS

The authors (A.A.R. and K.W.) would like to thank Professor M. O. Scully for his invitation and for the hospitality extended to them at the University of New Mexico, where this work has been done. K.W. would like to thank Professor J. Cooper for making available his papers prior to publication. A.A.R. would like to thank the United States Information Agency and the University Grants Commission, India for financial support. This work was partially supported by the Office of Naval Research.

*Permanent address: Department of Physics, University of Bombay, Bombay, 400-098, India.

†Permanent address: Institute of Theoretical Physics, Warsaw University, Warsaw 00-681, Poland.

¹See, for example, L. Allen and J. H. Eberly, *Optical Resonance and Two-Level Atoms* (Wiley, New York, 1975).

²K. Wódkiewicz and J. H. Eberly, *Phys. Rev. A* **32**, 992 (1985), and references therein.

³R. G. DeVoe and R. G. Brewer, *Phys. Rev. Lett.* **50**, 1269 (1983), and references therein.

⁴K. Wódkiewicz, *Phys. Rev. A* **19**, 1686 (1979).

⁵K. Wódkiewicz, *J. Math Phys.* **20**, 45 (1979).

⁶J. H. Eberly, *Phys. Rev. Lett.* **37**, 1387 (1976); G. S. Agarwal, *ibid.* **37**, 1383 (1976).

⁷M. H. Anderson, R. D. Jones, J. Cooper, S. J. Smith, D. S. Elliot, H. Ritsch, and P. Zoller, *Phys. Rev. Lett.* **64**, 1346 (1990).

⁸See, for example, P. Meystre and M. Sargent III, *Elements of*

Quantum Optics (Springer, New York, 1989), Chap. 15.

⁹Th. Haslwanter, H. Ritsch, J. Cooper, and P. Zoller, *Phys. Rev. A* **38**, 5652 (1988).

¹⁰K. Wódkiewicz, *Phys. Lett.* **77A**, 315 (1980); *J. Phys. B* **14**, L529 (1981).

¹¹H. Ritsch, P. Zoller, and J. Cooper, *Phys. Rev. A* **41**, 2653 (1990).

¹²The stochastic Mollow spectrum with amplitude fluctuations has been investigated in the following papers: F. Haake, J. W. Haus, and K. Rzążewski, *Z. Phys. B* **48**, 175 (1982); G. Vemuri, R. Roy, and G. S. Agarwal, *Phys. Rev. A* **41**, 2749 (1990).

¹³K. Wódkiewicz, *Phys. Lett.* **66A**, 369 (1978).

¹⁴D. L. Huber, *Phys. Rev.* **178**, 93 (1969).

¹⁵J. L. Carlsten, A. Szöke, and M. G. Raymer, *Phys. Rev. A* **15**, 1029 (1977).